Hybrid Control of the Buck Converter for Global Asymptotic Stabilization

Yusheng Fang and Ricardo G. Sanfelice[1]

***Abstract*— We consider the problem of globally controlling a DC-DC Buck converter. A constrained switched differential inclusion model is derived to capture all possible modes of operation of the Buck converter circuit. In contrast with the traditional pulse-width modulation control method, a control Lyapunov function-based controller is designed. A hybrid closed-loop system is formulated to combine the continuous dynamics of the converter circuit and the hybrid dynamics of the controller. The closed-loop system is proven to induce global stabilization of a desired output voltage setpoint. Simulations are provided to validate the results.**

I. Introduction

A key power-supplying component in every computing device is the DC-to-DC Buck converter, which supplies power to low-voltage devices. The Buck converter draws power from a DC voltage source and converts it to a lower DC voltage to supply power to a load. The industry standard control method for Buck converter consists of a pulse width modulator (PID) controller with pulse width modulation (PWM) output. However, this control method is known to have several drawbacks. First, the typical state-average modeling method only considers the linearized system dynamics in continuous conduction mode (CCM) at the vicinity around the steady-state operation point v^* (see Chapter 2 in [1]). Other dynamics, including capacitor charging before the steady state and discontinuous conduction mode (DCM) when the inductor current stays zero, are not captured. Second, in the typical PID control scheme, regulation of capacitor voltage and inductor current involves separate or cascaded control loops [2], adding complexity to the controller design. More recently, with the availability of enhanced computation power, nonlinear modeling techniques, including switched affine systems [3], sliding mode control [4], optimization-based control [5], and the hybrid modeling paradigm [6], [7], [8], have lead to provide more advanced control algorithms for power converter circuits.

In this paper, motivated by the need to achieve global stabilization of the Buck converter, we propose a state-space model that includes every possible mode of the converter, including the pre-charge mode and the DCM. A Control Lyapunov Function (CLF)-based controller, involving a reset law, is formulated to control the converter. Using hybrid system tools, a model of the closed-loop system is formulated and it is shown that the proposed controller induces global asymptotic stability of a desired operation point.

The remainder of the paper is organized as follows. In Section II, the switched dynamics of the Buck converter is modeled, and Krasovskii regularization is then performed to address the discontinuity between CCM and DCM. In Section III, the proposed CLF-based controller is designed, and the resulting closed-loop system is modeled as a hybrid system. In Section IV, the stability property of the hybrid closed-loop system is analyzed. Simulation results are presented in Section V. Due to space constraints, several proofs are omitted and will be included in future publications.

II. Modeling of the Buck Converter Circuit

A simplified single-switch DC-DC Buck converter circuit is shown in Figure 1. The circuit consists of a DC voltage source, an ideal switch, an ideal diode, an ideal inductor, an ideal capacitor, and a resistive load. The parameters are defined as follows: E is the voltage of the DC voltage source, L is the inductance of the inductor, C is the capacitance of the capacitor, and R is the resistance of the output load. In addition, the quantity $S \in \{0, 1\}$ indicates the state of the switch and $D \in \{0, 1\}$ indicates the state of the diode. The state of interest is defined as $x = (v_C, i_L)$, in which v_C is the voltage across the capacitor (it equals the output voltage v_O to the load), and i_L is the current through the inductor. We assume the output voltage and the inductor current values are instantaneously measurable.

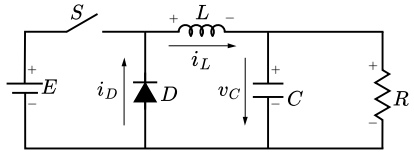

Fig. 1. Buck converter with ideal switch and ideal diode.

The dynamics of the circuit are determined by the values of S and D. Four modes of operations are defined as follows, where "1" represents the switch is closed or the diode is forward-biased, while "0" represents the switch is open or the diode is reverse-biased:

mode 1: $S = 1, D = 0$; mode 2: $S = 0, D = 1$;
mode 3: $S = 1, D = 1$; mode 4: $S = 0, D = 0$.

The circuit associated with each of the modes is depicted in Figure 2. Note that not every mode is valid. In mode 3, since $S = 1$, a negative voltage $-E$ from the voltage

[1]Yusheng Fang and Ricardo G. Sanfelice are with the Electrical and Computer Engineering Department, University of California, Santa Cruz, CA 95064. Email: yfang27@ucsc.edu, ricardo@ucsc.edu. Research by Ricardo G. Sanfelice is partially supported by NSF Grants no. CNS-2039054 and CNS-2111688, by AFOSR Grants nos. FA955019-1-0169, FA9550-20-1-0238, FA9550-23-1-0145, and FA9550-23-1-0313, by AFRL Grant nos. FA8651-22-1-0017 and FA8651-23-1-0004, by ARO Grant no. W911NF-20-1-0253, and by DoD Grant no. W911NF-23-1-0158.

source is applied to the diode. Therefore, it is reverse-biased ($D = 0$). Hence, mode 3 is not valid and is omitted from further analysis.

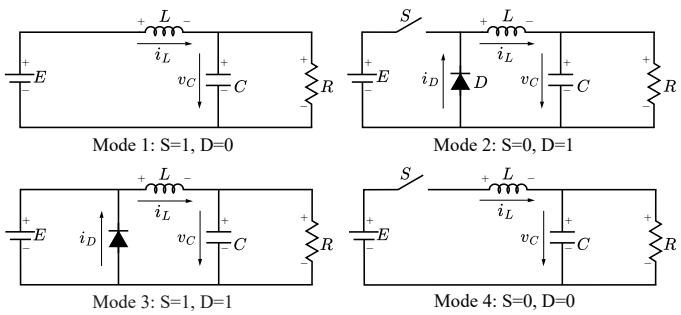

Fig. 2. Operation modes of the Buck converter.

In mode 1, the switch is closed (i.e., $S = 1$), and the diode is reverse-biased (i.e., $D = 0$). Using Kirchhoff's current law, the current flowing through the capacitor is given by $i_C = i_L - i_R$. Since $\dot{v_C} = \frac{i_C}{C}$ and $i_R = \frac{v_C}{R}$, we get the differential equation for v_C as $\dot{v_C} = \frac{i_L}{C} - \frac{v_C}{RC}$. By Kirchhoff's voltage law, the voltage across the inductor is given by $v_L = E - v_C = \dot{i_L}L$. Therefore, the state x evolves according to the differential equation

$$\begin{bmatrix} \dot{v_C} \\ \dot{i_L} \end{bmatrix} = \begin{bmatrix} \frac{i_L}{C} - \frac{v_C}{RC} \\ \frac{E}{L} - \frac{v_C}{L} \end{bmatrix} \tag{1}$$

In mode 2, the switch is open (i.e., $S = 0$) and the diode is forward-biased (i.e., $D = 1$). The voltage source E is disconnected from the circuit, the inductor L and the capacitor C start to discharge through the load resistor. Because the diode D only permits unidirectional current flow, the inductor current i_L evolves according to $\dot{i_L} = -\frac{v_C}{L}$ until it decreases to zero. Using the same derivation of $\dot{v_C}$ in mode 1, the state x is governed by

$$\begin{bmatrix} \dot{v_C} \\ \dot{i_L} \end{bmatrix} = \begin{bmatrix} \frac{i_L}{C} - \frac{v_C}{RC} \\ -\frac{v_C}{L} \end{bmatrix} \tag{2}$$

In mode 4, the switch is open (i.e., $S = 0$) and the diode is reverse-biased (i.e., $D = 0$). Current does not flow through the voltage source E and the inductor L; hence, the inductor current i_L is zero, and only the capacitor discharges through the load resistor R in this mode. Using Kirchhoff's current law, we have

$$\begin{bmatrix} \dot{v_C} \\ \dot{i_L} \end{bmatrix} = \begin{bmatrix} -\frac{v_C}{RC} \\ 0 \end{bmatrix} \tag{3}$$

Each mode has state constraints associated with it. In mode 1, to avoid counter electromotive-force at the voltage source E via that the capacitor C, the state x is constrained to $\{x \in \mathbb{R}^2 : 0 \leq v_C \leq E, i_L \geq 0\}$. In mode 2, since the diode D is forward-biased, the inductor current must satisfy $i_L = i_D \geq 0$. In mode 4, since the diode D is reverse-biased, the inductor current must satisfy $i_L = i_D = 0$. Therefore, $S = 1$ is only allowed when $x \in M_1 := \{x \in \mathbb{R}^2 : 0 \leq v_C \leq E, i_L \geq 0\}$, and $S = 0$ is only allowed when $x \in M_0 = M_2 \cup M_4$, where $M_2 := \{x \in \mathbb{R}^2 : v_C \geq 0, i_L > 0\}$ and $M_4 := \{x \in \mathbb{R}^2 : v_C \geq 0, i_L = 0\}$.

The dynamics of the complete circuit can be expressed as the switched differential equations

$$\dot{x} = f_S(x) \qquad x \in M_S, \tag{4}$$

where $S \in \{0, 1\}$ is treated as a control input and

$$f_0(x) := \begin{cases} \begin{bmatrix} \frac{i_L}{C} - \frac{v_C}{RC} \\ -\frac{v_C}{L} \end{bmatrix} & \forall\ x \in M_2 \\ \begin{bmatrix} -\frac{v_C}{RC} \\ 0 \end{bmatrix} & \forall\ x \in M_4 \end{cases}$$

$$f_1(x) := \begin{bmatrix} \frac{i_L}{C} - \frac{v_C}{RC} \\ \frac{E}{L} - \frac{v_C}{L} \end{bmatrix} \quad \forall\ x \in M_1$$

Note that for $S = 0$, the vector field is discontinuous at points in $\overline{M_2} \cap \overline{M_4} := \{x \in \mathbb{R}^2 : v_C \geq 0, i_L = 0\}$, which is a set of measure zero. To cope with this discontinuity, Krasovskii regularization [9] is performed to obtain a differential inclusion with a regular right-hand side, as follows:

1) For $S = 0$, the regularized set for the evolution of the state x is $\widetilde{M_0} := \overline{M_2 \cup M_4} = \{x \in \mathbb{R}^2 : v_C \geq 0, i_L \geq 0\}$.
2) For $S = 1$, the regularized set is $\widetilde{M_1} := \overline{M_1} = \{x \in \mathbb{R}^2 : 0 \leq v_C \leq E, i_L \geq 0\}$.
3) The regularization of f_0 is given by, for each $x \in \widetilde{M_0}$,

$$\begin{aligned} F_0(x) &:= \bigcap_{\delta > 0} \overline{\text{co}} f_0 \left((x + \delta \mathbb{B} \cap \widetilde{M_0}) \right) \\ &= \begin{cases} \begin{bmatrix} \frac{i_L}{C} - \frac{v_C}{RC} \\ -\frac{v_C}{L} \end{bmatrix} & \text{if } x \in M_2 \\ \{-\frac{v_C}{RC}\} \times [-\frac{v_C}{L}, 0] & \text{if } x \in M_4 \end{cases} \end{aligned} \tag{5}$$

4) Since f_1 is continuous, the regularization leads to

$$F_1(x) = \{f_1(x)\} \qquad \forall\ x \in \widetilde{M_1} \tag{6}$$

The resulting system is a switched differential inclusion with constraints, given as

$$\dot{x} \in F_S(x) \qquad \forall\ x \in \widetilde{M_S} \tag{7}$$

With this constrained switched differential inclusion model that captures the complete dynamics of the Buck converter circuit, we are ready to design a CLF-based controller.

III. CLF-Based Controller Design

In this section, unlike the traditional PID controller with a duty-cycle driven PWM output, we formulate a CLF-based controller by defining a state-dependent switching law. This reset law involves the reference voltage v^*, the position of the switch S, the output voltage v_O, and the inductor current i_L to define the value of the control input S.

A. Control Lyapunov Function

We follow the approach in [10] to identify a quadratic CLF candidate. For a Buck converter with input voltage source E and load R, let the commanded setpoint be

$$x^* = (v_C^*, i_L^*) = \left(v_C^*, \frac{v_C^*}{R}\right).$$

Note that rather than being arbitrary, the commanded inductor current i_L^* is selected to equal the steady state inductor current so that the average capacitor current is zero.

Consider the CLF candidate

$$V(x) = (x - x^*)^T P (x - x^*) \tag{8}$$

in which $P = \left[\begin{smallmatrix} p_{11} & 0 \\ 0 & p_{22} \end{smallmatrix}\right] > 0$. To characterize the change of V along flows, we proceed as follows:

- For $S = 0$ and each $x \in M_2$, $F_0(x) = \begin{bmatrix} \frac{i_L}{C} - \frac{v_C}{RC} \\ -\frac{v_C}{L} \end{bmatrix}$,

$$\begin{aligned}\langle \nabla V(x), F_0(x) \rangle = 2p_{11}(v_C - v_C^*)\left(\frac{i_L}{C} - \frac{v_C}{RC}\right) \\ + 2p_{22}(i_L - i_L^*)\left(-\frac{v_C}{L}\right).\end{aligned} \tag{9}$$

- For $S = 0$ and $x \in M_4$, since $F_0(x) = \{-\frac{v_C}{RC}\} \times \left[-\frac{v_C}{L}, 0\right]$ is a set, we have

$$\begin{aligned}&\max_{\xi \in F_0(x)} \langle \nabla V(x), \xi \rangle = \\ &\max_{\xi_2 \in \left[-\frac{v_C}{L}, 0\right]} \left\langle \nabla V(x), \left\{-\frac{v_C}{RC}\right\} \times \{\xi_2\} \right\rangle = \\ &\begin{cases} 2p_{11}(v_C - v_C^*)\left(-\frac{v_C}{RC}\right) + 2p_{22}(i_L - i_L^*)\left(-\frac{v_C}{L}\right) \\ \qquad\qquad\qquad\qquad \text{if } i_L < i_L^*, \\ 2p_{11}(v_C - v_C^*)\left(-\frac{v_C}{RC}\right) \qquad \text{if } i_L \geq i_L^*. \end{cases}\end{aligned}$$

Since for $x \in M_4$, $i_L = 0$ and $i_L^* > 0$, inequality $i_L \geq i_L^*$ would never happen, we conclude that for $S = 0$ and each $x \in M_4$,

$$\begin{aligned}\max_{\xi \in F_0(x)} \langle \nabla V(x), \xi \rangle = 2p_{11}(v_C - v_C^*)\left(-\frac{v_C}{RC}\right) \\ + 2p_{22}(i_L - i_L^*)\left(-\frac{v_C}{L}\right).\end{aligned} \tag{10}$$

- For $S = 1$ and each $x \in M_1$, $F_1(x) = \begin{bmatrix} \frac{i_L}{C} - \frac{v_C}{RC} \\ \frac{E}{L} - \frac{v_C}{L} \end{bmatrix}$,

$$\begin{aligned}\langle \nabla V(x), F_1(x) \rangle = 2p_{11}(v_C - v_C^*)\left(\frac{i_L}{C} - \frac{v_C}{RC}\right) \\ + 2p_{22}(i_L - i_L^*)\left(\frac{E - v_C}{L}\right).\end{aligned} \tag{11}$$

Notice that the expressions in (9) and (10) are equal thus can be combined. Then, for each $x \in \mathbb{R}^2$, we define functions γ_0 and γ_1 as

$$\begin{aligned}\gamma_0(x) &:= 2p_{11}(v_C - v_C^*)\left(\frac{i_L}{C} - \frac{v_C}{RC}\right) + \\ &\qquad 2p_{22}(i_L - i_L^*)\left(-\frac{v_C}{L}\right), \\ \gamma_1(x) &:= 2p_{11}(v_C - v_C^*)\left(\frac{i_L}{C} - \frac{v_C}{RC}\right) + \\ &\qquad 2p_{22}(i_L - i_L^*)\left(\frac{E - v_C}{L}\right)\end{aligned} \tag{12}$$

and conclude that

$$\max_{\xi \in F_S(x)} \langle \nabla V(x), \xi \rangle = \begin{cases} \gamma_0(x) & \text{if } S = 0, x \in \widetilde{M}_0 \\ \gamma_1(x) & \text{if } S = 1, x \in \widetilde{M}_1. \end{cases} \tag{13}$$

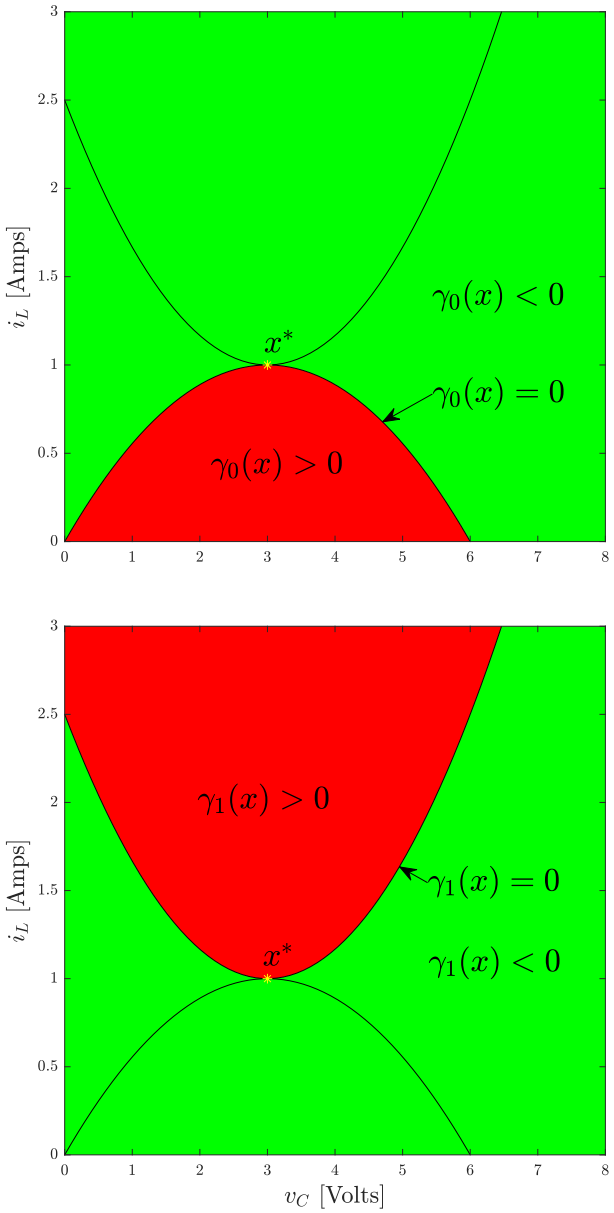

Fig. 3. Switch boundaries of $\gamma_0(x) = 0$ (left) and $\gamma_1(x) = 0$ (right) for a Buck Converter circuit.

The functions γ_0 and γ_1 in (12) are similar to the functions defined in [11]. The zero level contours of $\gamma_0(x) = 0$ and $\gamma_1(x) = 0$ are plotted in Fig. 3. Since these functions provide an upper bound on the inner product between the gradient of V and the flow of F_S, the following lemma establishes that V is a CLF and that γ_0 and γ_1 can be used to define a state-dependent switching control law to assign the control input S.

Lemma 1. *Let $E, R, p_{11}, p_{22} > 0$, $\frac{p_{11}}{C} = \frac{p_{22}}{L}$, $v_C^* < E$, $i_L^* = \frac{v_C^*}{R}$, and $\mathcal{A}_x := \{x \in \mathbb{R}^2 : v_C = v_C^*, i_L = i_L^*\}$. The following properties hold:*

1) *For each $x \in \mathbb{R}^2 \setminus \mathcal{A}_x$, there exists $S \in \{0, 1\}$ such that $\gamma_S(x) < 0$.*
2) *For each $x \in \mathcal{A}_x$ and each $S \in \{0, 1\}$, $\gamma_S(x) = 0$.*

B. Controller Design

Based on the properties derived in Lemma 1, we can derive a control law to stabilize the desired setpoint $\mathcal{A}_x$. The state-dependent law used to assign the control input S is defined as

$$S = \underset{S\in\{0,1\}}{\arg\min} \underset{\xi\in F_S(x)}{\arg\max} \langle \nabla V(x), \xi \rangle \tag{14}$$

To model the closed-loop system, we define the combined state of the circuit and the controller as (x, S). Using the definition in Lemma 1, the control logic is defined as follows:

- The logic-based control law selects the control input S based on the current value of the state S of the switch and the value of the state x of the circuit.
- The control input S remains the same as long as $\gamma_S(x) < 0$.
- The control input S switches to $1 - S$ once $\gamma_S(x) = 0$. As observed in Figure 3, for $S \in \{0, 1\}$ and $x \in \mathbb{R}^2 \setminus \mathcal{A}_x$, $\gamma_S(x) \geq 0$ implies $\gamma_{1-S}(x) \leq 0$.
- The change of S guarantees that the CLF V decreases along solutions with initial conditions for $x \notin \mathcal{A}_x$.
- The state x stays in $\mathcal{A}_x$ once it reaches $\mathcal{A}_x$.

Using the hybrid modeling method in [12], the control logic above can be expressed as follows

$$\begin{aligned} \dot{S} &= 0 && \text{if } \gamma_S(x) \leq 0 \\ S^+ &= 1 - S && \text{if } \gamma_S(x) = 0 \end{aligned} \tag{15}$$

C. Hybrid Closed-Loop System

Following the hybrid modeling method in [12], we combine the proposed CLF-based controller with the model of the Buck converter circuit. Due to the continuous dynamics of the model of the Buck converter circuit and the dynamics of the logic controller, we model the closed-loop system as a hybrid system $\mathcal{H} = (C, F, D, G)$ given by

$$\begin{aligned} \begin{bmatrix} \dot{x} \\ \dot{S} \end{bmatrix} &\in F(x, S) := \begin{bmatrix} F_S(x) \\ 0 \end{bmatrix} && (x, S) \in C \\ \begin{bmatrix} x^+ \\ S^+ \end{bmatrix} &= G(x, S) := \begin{bmatrix} x \\ 1 - S \end{bmatrix} && (x, S) \in D \end{aligned} \tag{16}$$

where

$$\begin{aligned} C =& \{(x, S) : x \in \widetilde{M}_S, \gamma_S(x) \leq 0\} \\ D =& \{(x, S) : x \in \widetilde{M}_S, \gamma_S(x) = 0\} \end{aligned} \tag{17}$$

in which

$$\begin{aligned} \widetilde{M}_0 &= \overline{M_2 \cup M_4} = \{x \in \mathbb{R}^2 : v_C \geq 0, i_L \geq 0\} \\ \widetilde{M}_1 &= \overline{M_1} = \{x \in \mathbb{R}^2 : 0 \leq v_C \leq E, i_L \geq 0\} \end{aligned} \tag{18}$$

The flow map F in (16) stacks the flow map of the Buck converter circuit dynamics (7) with zero, in the sense that when the hybrid closed-loop system flows, the state x is determined by the dynamics of the circuit while S remains constant. The jump map G indicates that the state x does not change at jumps, and the switch toggles its position S to $1 - S$ at jumps. Note that the selection of the sets C and D in (17) is not arbitrary. By combining the constraints of the switching boundaries defined by the zero level sets $\gamma_S(x) = 0$ and the operational range $\widetilde{M}_S$ of each mode of the Buck converter circuit, the CLF along solutions to the hybrid closed-loop system decreases as the state x approaches the setpoint x^*.

IV. Properties of the Hybrid Closed-Loop System

A. Basic Properties

The hybrid closed-loop system $\mathcal{H}$ in (16) satisfies the hybrid basic conditions; hence, from Theorem 6.8 in [12], it is well-posed.

Proposition 2. *The hybrid system $\mathcal{H}$ given by (16) satisfies the hybrid basic conditions, namely:*

- (A1) *C and D are closed subsets of $\mathbb{R}^n$;*
- (A2) *$F : \mathbb{R}^n \rightrightarrows \mathbb{R}^n$ is outer semicontinous and locally bounded relative to C, $C \subset$ dom F, and $F(x)$ is convex for every $x \in C$;*
- (A3) *$G : \mathbb{R}^n \rightrightarrows \mathbb{R}^n$ is outer semicontinous and locally bounded relative to D, and $D \subset$ dom G.*

Next, using Proposition 6.10 in [12], every solution to $\mathcal{H}$ in 16 such that it is not a truncation of another solution, which is said to be maximal, can be certified to be complete; namely, the domain of each maximal solution is unbounded.

Proposition 3. *For each $\xi \in C \cup D$, every maximal solution $\phi = (x, S)$ to the hybrid closed-loop system $\mathcal{H}$ given by (16) with $\phi(0, 0) = \xi$ is complete.*

B. Stability of the Hybrid System

We apply the invariance principle in Theorem 8.2 from [12] to certify global asymptotic stability of the setpoint x^* for $\mathcal{H}$ in (16)

Proposition 4. *For the hybrid system $\mathcal{H}$ in (16) with parameters $E, R, p_{11}, p_{22} > 0$, $\frac{p_{11}}{C} = \frac{p_{22}}{L}$, $v_C^* < E$, $i_L^* = \frac{v_C}{R}$, and $\mathcal{A}_x = \{x \in \mathbb{R}^2 : v_C = v_C^*, i_L = i_L^*\}$, the compact set*

$$\mathcal{A} := \mathcal{A}_x \times \{0, 1\} \tag{19}$$

is globally asymptotically stable for $\mathcal{H}$; namely, the compact set $\mathcal{A}$ is stable, meaning that for every $\epsilon > 0$ there exists $\delta > 0$ such that every solution (x, S) with $|(x(0, 0), S(0, 0))|_{\mathcal{A}} \leq \delta$ satisfies $|(x(t, j), S(t, j))|_{\mathcal{A}} \leq \epsilon$ for all $(t, j) \in$ dom(x, S), and globally attractive, meaning that every maximal solution (x, S) satisfies $\lim_{t+j\to\infty} |(x(t, j), S(t, j))|_{\mathcal{A}} = 0$.

C. Spatial Regularization to avoid Zeno Behavior

In the proposed CLF-based controller design, the switching frequency increases as the state x approaches the desired setpoint $\mathcal{A}_x$. The next section presents a simulation showing that, see Section V-A. To address this issue, given $\rho \in \mathbb{R}_{>0}$, the switch boundaries are now modified to be $\gamma_0 = \rho$ and $\gamma_1 = \rho$, we only allow switches of S when $\gamma_S(x) = \rho$. The resulting system, which can be considered as a spatially regularized system, denoted as $\mathcal{H}^\rho = (C_\rho, F, D_\rho, G)$, is given by

$$\begin{aligned} \begin{bmatrix} \dot{x} \\ \dot{S} \end{bmatrix} &\in F(x,S) := \begin{bmatrix} F_S(x) \\ 0 \end{bmatrix} \qquad (x,S) \in C_\rho \\ \begin{bmatrix} x^+ \\ S^+ \end{bmatrix} &= G(x,S) := \begin{bmatrix} x \\ 1-S \end{bmatrix} \qquad (x,S) \in D_\rho \end{aligned} \tag{20}$$

where

$$\begin{aligned} C_\rho := &\{(x,S) : x \in \widetilde{M}_0, \gamma_0(x) \le \rho, S = 0\} \cup \\ &\{(x,S) : x \in \widetilde{M}_1, \gamma_1(x) \le \rho, S = 1\}, \\ D_\rho := &\{(x,S) : x \in \widetilde{M}_0, \gamma_0(x) = \rho, S = 0\} \cup \\ &\{(x,S) : x \in \widetilde{M}_1, \gamma_1(x) = \rho, S = 1\}. \end{aligned}$$

With the revised switching logic, no Zeno behavior occurs since the switching boundaries $\gamma_0(x) = \rho$ and $\gamma_1(x) = \rho$ do not intersect and have a minimum distance of 2ρ. Therefore, the switching frequency is reduced, however, at the cost of increased error between the setpoint x^* and the state x. A simulation of the spatially regularized system is presented in section V-B.

V. Simulation of the Hybrid Closed-Loop System

In this section, several simulation results[1] of the hybrid closed-loop system are presented using the Hybrid Equation Toolbox [13]. The simulations are performed using parameters $E = 5\ V, R = 3\ \Omega, C = 0.1\ F, L = 0.05\ H, p_{11} = \frac{C}{2}, p_{22} = \frac{L}{2}, x^* = (v_C^*, i_L^*) = (3,1)$, unless specified otherwise.

A. Discontinuous and Continuous Conduction Modes

In Figure 4, three simulations are plotted in the same charts. The blue color trajectory corresponds to the DCM, while the red and cyan color trajectories correspond to CCM.

We first demonstrate that the discontinuous conduction mode is included in the control scheme. As seen in the blue trajectory, from the initial conditions $x_0 = (7,2), S_0 = 1$, the constraints in $\widetilde{M}_1$ render the state jump to $S = 0$ immediately; the inductor current then starts to decrease till it reaches zero; due to the existence of the diode, the inductor current remains zero till the capacitor voltage falls into the operational range of Buck converter $v_C \in [0, E]$; once v_C reaches E, S switches to 1; after that, the CLF-based controller starts to steer the state to the commanded setpoint. The inclusion of the discontinuous conduction mode shows the global stabilization capability of the hybrid modeling scheme.

[1]Matlab script can be accessed at `https://github.com/HybridSystemsLab/BuckConverter`

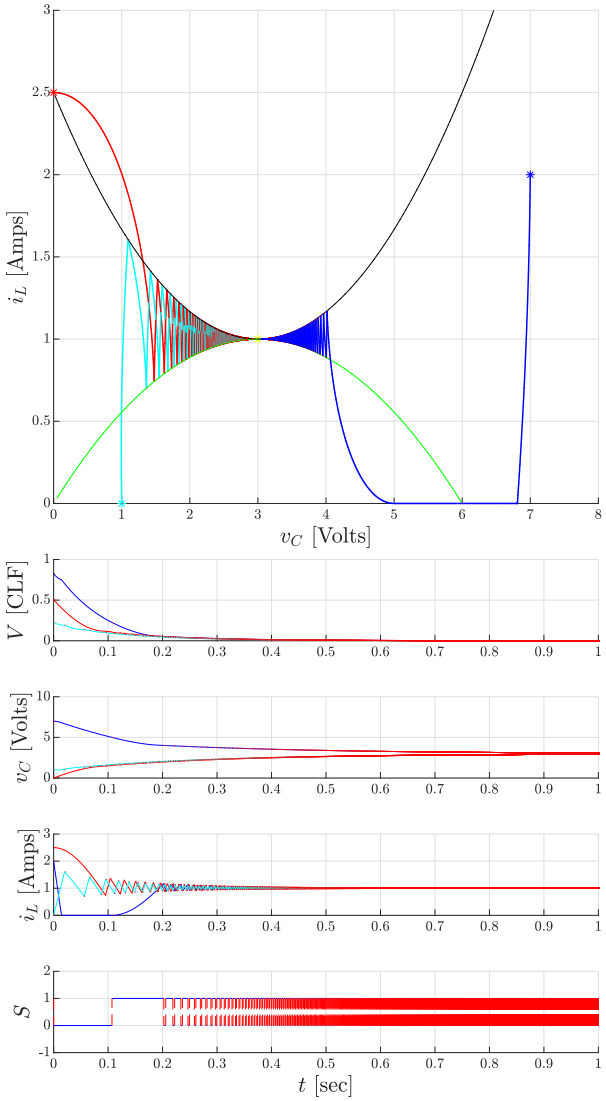

Fig. 4. Simulation results for the closed-loop system $\mathcal{H}$ from 3 initial conditions. The left subplot is the trajectory of the state $x = (v_C, i_L)$; on the right, four subplots are the evolutions of the value of the CLF V, capacitor voltage v_C, inductor current i_L, and the position S of the switch, from top to bottom respectively. Note the switch position plot only includes the evolution in DCM to avoid overlapping; the blue horizontal solid line indicates the switch keeps its position so that the hybrid system flows, while the red vertical dashed line indicates the switch toggles its position at which the hybrid system jumps.

The hybrid closed-loop system can also handle normal CCM operation. From initial conditions $x_0 = (1,0), S_0 = 0$ and $x_0 = (0,2.5), S_0 = 1$, we can see the state of the circuit converges to the commanded setpoint. Note that for all three scenarios, the value of the CLF V strictly decreases along the trajectory of the state x, which exhibits the asymptotic stabilization capability of the controller.

B. Spatially Regularized Hybrid System

In Figure 5, we simulate the spatially regularized system as in (20). Three simulations from the same initial conditions

as in the previous section are plotted. With the spatial regularization parameter $\rho = 0.2$, the two parabolas representing the switch boundaries are apart with a distance of 2ρ. The switch toggles less often, at the cost that the error $|x - x^*|$ increases.

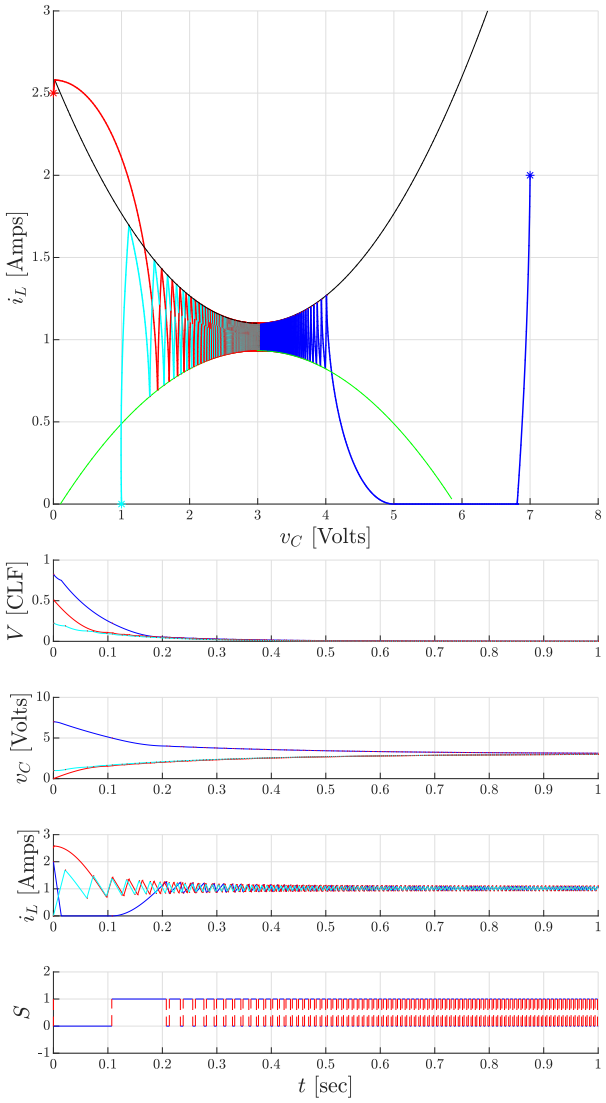

Fig. 5. Simulation results for the spatial regularized hybrid system $\mathcal{H}^\rho$ with the same initial conditions and spatial regularization parameter $\rho = 0.2$.

Conclusion

In this paper, a hybrid model of the closed-loop Buck converter circuit is obtained. This constrained switched model with a discontinuous right-hand side includes all possible modes of the Buck Converter circuit. A CLF-based controller is designed using a state-dependent switching method. It is demonstrated that asymptotic global stabilization can be achieved by combining the CLF-based controller and the switched modeling of the converter circuit. Compared to the traditional control method, which could only attain steady mode operation, this state-dependent switching law could also handle scenarios including pre-charge mode and discontinuous conduction mode.

Future work includes further investigating the technique to modify the switching boundaries and the relationship between spatial regulation and steady-state error. Also note that in this paper, we assume that the supply voltage E and the load resistance R are accessible and constant, which is not always the case; an estimation algorithm of these parameters will be proposed in future publications.

References

[1] R. W. Erickson and D. Maksimović, *The Discontinuous Conduction Mode*, pp. 135–162. Cham: Springer International Publishing, 2020.

[2] M. Ishaq, M. Waqar, and M. H. Afzal, "Design of double closed-loop boost converter controller to reduce transient voltage dip for sudden load connection," in *2023 International Conference on Emerging Power Technologies (ICEPT)*, pp. 1–5, 2023.

[3] X. Xu, Y. Zhu, F. Wu, and C. K. Ahn, "Sampled-data control for buck-boost converter using a switched affine systems approach," *IEEE Transactions on Circuits and Systems I: Regular Papers*, vol. 71, no. 7, pp. 3380–3389, 2024.

[4] S. Mobayen, F. Bayat, C.-C. Lai, A. Taheri, and A. Fekih, "Adaptive global sliding mode controller design for perturbed dc-dc buck converters," *Energies*, vol. 14, no. 5, 2021.

[5] Z. Karami, Q. Shafiee, S. Sahoo, M. Yaribeygi, H. Bevrani, and T. Dragicevic, "Hybrid model predictive control of dc–dc boost converters with constant power load," *IEEE Transactions on Energy Conversion*, vol. 36, no. 2, pp. 1347–1356, 2021.

[6] M. Senesky, G. Eirea, and T. J. Koo, "Hybrid modelling and control of power electronics," in *Hybrid Systems: Computation and Control* (O. Maler and A. Pnueli, eds.), (Berlin, Heidelberg), pp. 450–465, Springer Berlin Heidelberg, 2003.

[7] T. Geyer, G. Papafotiou, and M. Morari, "On the optimal control of switch-mode dc-dc converters," in *Hybrid Systems: Computation and Control* (R. Alur and G. J. Pappas, eds.), (Berlin, Heidelberg), pp. 342–356, Springer Berlin Heidelberg, 2004.

[8] F. Vasca, L. Iannelli, M. K. Camlibel, and R. Frasca, "A new perspective for modeling power electronics converters: Complementarity framework," *IEEE Transactions on Power Electronics*, vol. 24, pp. 456–468, Feb 2009.

[9] R. G. Sanfelice, R. Goebel, and A. R. Teel, "Generalized solutions to hybrid dynamical systems," *ESAIM: Control, Optimisation and Calculus of Variations*, vol. 14, no. 4, p. 699–724, 2008.

[10] E. D. Sontag, "A lyapunov-like characterization of asymptotic controllability," *SIAM Journal on Control and Optimization*, vol. 21, no. 3, pp. 462–471, 1983.

[11] T. A. F. Theunisse, J. Chai, R. G. Sanfelice, and W. P. M. H. Heemels, "Robust global stabilization of the dc-dc boost converter via hybrid control," *IEEE Transactions on Circuits and Systems I: Regular Papers*, vol. 62, no. 4, pp. 1052–1061, 2015.

[12] R. Goebel, R. G. Sanfelice, and A. R. Teel, *Hybrid Dynamical Systems: Modeling, Stability, and Robustness*. Princeton University Press, 03 2012.

[13] R. G. Sanfelice, D. Copp, and P. Nanez, "A toolbox for simulation of hybrid systems in matlab/simulink: hybrid equations (hyeq) toolbox," in *Proceedings of the 16th International Conference on Hybrid Systems: Computation and Control*, HSCC '13, (New York, NY, USA), p. 101–106, Association for Computing Machinery, 2013.